ACCSCIENCE PUBLISHING

Eurasian Journal of Medicine and Oncology

ORIGINAL RESEARCH ARTICLE

Machine learning-based screening of anoikis-related genes in melanoma diagnosis and their clinicopathological significance

Tengfei Wang[1] and Jinchao Zhu[2]*

[1]Department of Pathology, Funan County People's Hospital, Fuyang City, Anhui, China

[2]Department of Pathology, The Ninth People's Hospital, Shanghai Jiao Tong University School of Medicine, Shanghai, China

Abstract

Introduction: Cutaneous melanoma, a highly aggressive malignant tumor, continues to pose significant challenges in early diagnosis and prognosis assessment. Although anoikis-related genes (ARGs) play crucial roles in tumor progression, systematic molecular diagnostic biomarkers remain lacking.

Objective: This study aims to elucidate the molecular mechanisms and diagnostic value of ARGs in cutaneous melanoma using advanced bioinformatics and machine learning approaches.

Methods: Multiple melanoma datasets from The Cancer Genome Atlas and GEO databases (GSE3189, GSE15605, GSE19234, GSE65904, and GSE66839) were integrated to analyze ARG expression patterns. Differential expression analysis identified candidate genes significantly associated with cutaneous skin melanoma. A total of 113 machine learning models were employed to screen and validate candidate genes, with receiver operating characteristic curves evaluating diagnostic value. Core genes were identified through protein-protein interaction (PPI) networks. The immune infiltration correlations of core genes were analyzed, and their tissue-level expression was validated using immunohistochemistry.

Results: Twenty-two ARGs were significantly enriched in cancer signaling pathways, including phosphoinositide 3-kinase-protein kinase B, hypoxia-inducible factor 1, and programmed death-ligand 1. Nine candidate genes were identified through differential and intersection analysis, and eight model genes were further screened using machine learning. Seven genes exhibited high diagnostic efficacy in both training and external validation sets (area under the curve [AUC] >0.7). Survival analysis revealed that high expression of carcinoembryonic antigen-related cell adhesion molecule (*CEACAM)5*, *CEACAM6*, epidermal growth factor receptor (*EGFR*), stratifin (*SFN)*, and Polo-like kinase 1 (*PLK1*) correlated with poor prognosis. PPI analysis confirmed these as core regulatory factors, and immune infiltration analysis revealed strong associations with dendritic cells, T cells, and macrophages. The five-gene combination yielded excellent diagnostic performance, with AUCs of 0.969 (training) and 0.971 (validation). Immunohistochemistry confirmed their elevated expression in melanoma tissues.

Conclusion: This study identified five key *ARGs*, *CEACAM5*, *CEACAM6*, *EGFR*, *SFN*, and *PLK1*, as significantly upregulated in cutaneous melanoma and associated with poor prognosis. Their combined diagnostic power suggests strong potential as clinical pathological biomarkers.

Keywords: Machine learning; Immunohistochemistry; Biomarkers; Melanoma; Anoikis

***Corresponding author:**
Jinchao Zhu
(211300147@st.usst.edu.cn)

Citation: Wang T, Zhu J. Machine learning-based screening of anoikis-related genes in melanoma diagnosis and their clinicopathological significance. *Eurasian J Med Oncol*. 2026;10(3):025220218. doi: 10.36922/EJMO025220218

Received: May 26, 2025

Revised: June 26, 2025

Accepted: July 9, 2025

Published online: August 12, 2025

1. Introduction

Melanoma is a malignant tumor arising from melanocytes or melanocyte-like cells in the skin, characterized by its highly invasive and metastatic capabilities.[1] The main subtypes of this oncological pathology comprise superficial spreading melanoma (70% of cases), nodular melanoma (5%), lentigo maligna melanoma (4–15%), acral lentiginous melanoma (5%), amelanotic melanoma (4%), and desmoplastic melanoma (<4%).[2] Epidemiological data indicate that the incidence of melanoma continues to rise.[3] Men are approximately 1.5 times more likely to develop melanoma than women. However, studies examining age-specific incidence rates show that women have higher incidence rates before the age of 40 years, whereas by the age of 75 years, the incidence in men is nearly three times higher than in women.[4] While the incidence of numerous other tumor types is declining, melanoma rates continue to increase.[5] This persistent rise has become a significant socioeconomic concern, with the average lifetime risk of developing melanoma reaching as high as 50%.[6]

Despite recent advances in cancer treatment, melanoma treatment still faces enormous challenges. Research by Tumeh *et al.*[7] indicates that the response rates to current targeted therapy and immunotherapies are only 7–12%, highlighting the urgent need for deeper investigation into the mechanisms of melanoma pathogenesis. One of the major challenges is the more accurate and therapeutically predictive identification of patient populations likely to benefit from specific interventions.

Anoikis is a form of programmed cell death triggered by the loss of attachment to the extracellular matrix, and it plays a crucial role in tumor development.[8,9] Frisch and Screaton[10] elaborated that anoikis serves as an important barrier to cancer cell metastasis by inducing cell death when extracellular matrix support is lost. Alterations in certain molecules/pathways have been associated with resistance to anoikis in metastatic cancers.[11] Anoikis is essential for both development and tissue homeostasis, and studies suggest that this pathway can suppress tumor cell formation.[12] During tumor progression, anoikis plays a critical role, as cancer cells must overcome their dependence on surrounding tissues to acquire metastatic potential.

Anoikis resistance is a key mechanism supporting the growth and spread of numerous malignant tumors. In cancer cells, anti-anoikis pathways such as phosphoinositide 3-kinase (PI3K)/protein kinase B (Akt) are often activated, for example, epidermal growth factor (EGF)-like domain-containing protein 7 regulates colorectal cancer cell invasion and anoikis through the PI3K/AKT pathway.[13] Similarly, nuclear factor kappa-light-chain-enhancer of activated B cell (NF-κB) activation, driven by inhibitor of κB (IκB) degradation and IκB kinase activity,[14] plays a crucial role in anoikis regulation. IκBs retain NF-κB in the cytoplasm, preventing its nuclear entry and maintaining its inactive state.[15] Therefore, a comprehensive understanding of anoikis is necessary for elucidating melanoma progression, metastasis, and chemotherapy resistance.

Despite its well-established importance in tumor biology, the diagnostic potential of anoikis in melanoma remains underexplored. Current pathological diagnosis of melanoma primarily relies on morphological assessment and a limited set of molecular markers, such as S100, human melanoma black (HMB)-45, and melanoma antigen A (Melan-A), which lack specificity in certain atypical cases and may lead to diagnostic ambiguity or misdiagnosis, particularly in early or borderline lesions. This underscores the urgent need for more precise molecular diagnostic tools.

This study aims to systematically identify key anoikis-related genes (ARGs) involved in melanoma using various machine learning algorithms, thereby establishing a novel pathological diagnostic marker system. By integrating transcriptomic data from multiple public databases, and combining differential expression analysis, multi-model machine learning screening, receiver operating characteristic (ROC) curve assessment, and protein-protein interaction (PPI) network analysis, we comprehensively evaluate the diagnostic value of ARGs in melanoma. Furthermore, immunohistochemical validation confirms the tissue-level expression of the identified key genes, providing an experimental basis for their clinical application. This study therefore holds significant scientific and translational potential for improving diagnostic accuracy and patient outcomes in melanoma.

2. Materials and methods

2.1. Gene expression profile data sources and processing

Skin cutaneous melanoma (SKCM) datasets were obtained from The Cancer Genome Atlas (TCGA), including transcriptomic matrices and clinical information for (SKCM; n = 471) and normal tissue (n = 1). Normal skin tissue expression data were sourced from the Genotype-Tissue Expression (GTEx) portal (https://gtexportal.org/home/). The GSE3189, GSE15605, GSE19234, GSE65904, and GSE66839 datasets, all containing available overall survival (OS) data, were retrieved from the public Gene Expression Omnibus database. RNA expression data were converted to transcripts per million. Somatic mutation and copy number variation (CNV) data were also obtained from TCGA. The GSE3189 and GSE15605 datasets were

merged using the R package "sva" (Bioconductor, USA) after batch effect removal. ARGs were obtained from GeneCards (https://www.genecards.org/).

2.2. Differential expression gene analysis and data intersection

Differentially expressed genes (DEGs) between the SKCM and control groups were identified using the R package "limma." The criteria for significance were |log2 fold change (log2FC)| ≥1.5 and an adjusted $p<0.05$. Univariate Cox regression analysis was then performed to screen ARGs with prognostic risk potential. The intersection of DEGs and ARGs was subsequently identified to obtain overlapping genes.

2.3. Gene ontology (GO) and Kyoto Encyclopedia of Genes and Genomes (KEGG) pathway enrichment analysis

GO and KEGG pathway enrichment analyses were conducted on the overlapping genes to explore their functional roles in SKCM. The R packages "clusterProfiler," "DOSE," and "org.Hs.eg.db" were systematically used for the enrichment analyses. A $p<0.05$ was considered the threshold for identifying significantly enriched terms.

2.4. Feature selection through machine learning-based integration

Feature selection was performed on the overlapping genes between DEGs and ARGs using a machine learning-based integration approach. Twelve machine learning models were employed—Ridge, Gradient Boosting Machine, Support Vector Machine, Linear Discriminant Analysis, Random Forest, Least Absolute Shrinkage and Selection Operator, Stepwise Generalized Linear Model, Elastic Net, Partial Least Squares Regression for Generalized Linear Models, Extreme Gradient Boosting, Naive Bayes, and Generalized Linear Model Boosting—generating a total of 113 algorithmic combinations. All model combinations were evaluated in both training and testing cohorts. Model performance was evaluated using the area under the curve (AUC) score. The model with the highest average AUC in both cohorts was considered optimal, and feature genes were identified from this best-performing model.

2.5. Diagnostic capability assessment, prognostic analysis, and PPI of model genes

To explore the diagnostic and prognostic value of specific genes in SKCM, rigorous bioinformatics analyses were performed. First, the diagnostic efficacy of key genes was comprehensively evaluated using ROC analysis with the R packages "glmnet" and "pROC." Genes demonstrating strong diagnostic performance (AUC >0.7) in independent testing and validation sets were considered potential core biomarkers, offering valuable insights for precise SKCM diagnosis. Prognostic analysis of these core genes was then carried out using the R package "survival" to examine associations between gene expression and patient survival outcomes, providing scientific evidence to support personalized SKCM treatment strategies. PPI analysis of the model genes was performed using the STRING database (https://string-db.org/), and hub genes were identified with Cytoscape software (Cytoscape Consortium, USA).

2.6. Correlation analysis between model genes and immune cell infiltration

To investigate the correlation between model genes and immune cell infiltration, CIBERSORT (Stanford University School of Medicine, USA) was used to calculate associations between immune-infiltrating cells and model gene expression. CIBERSORT is a bioinformatics tool based on gene expression data that quantitatively assesses the proportions of different immune cell types in tissue samples. The relationships between model genes and immune-infiltrating cells were identified through CIBERSORT analysis.

2.7. Combined ROC analysis of model genes and nomogram construction

To comprehensively assess the synergistic diagnostic potential of core genes in SKCM, in-depth multidimensional analyses were performed. Using the R packages "pROC" and "glmnet," a refined combined ROC analysis was conducted on the screened core genes to systematically evaluate their collective diagnostic performance. GSE15605 and GSE3189 were used as testing sets, while GSE46517 served as the validation set. Additionally, to further investigate the unique diagnostic value of each gene, clinical prediction nomograms were constructed using the "rms" and "rmda" packages. This approach not only illustrates the relative weights and contributions of individual genes but also provides intuitive tools for risk prediction and auxiliary clinical decision-making.

2.8. Immunohistochemical analysis of core gene proteins

To validate the protein expression patterns of core genes in SKCM tissues, rigorous histological detection was conducted. The experimental procedures included the use of standard paraffin-embedding techniques for the precise processing of SKCM tissue specimens. After systematic dehydration, tissues were embedded in paraffin and sectioned into thin slices. These sections were then subjected to high-temperature baking to ensure stability and enhance staining quality. Both routine hematoxylin

and eosin staining and specific immunohistochemical staining were performed. For immunohistochemical staining, the following primary antibodies were used: anti-carcinoembryonic antigen-related cell adhesion molecule 5 (CEACAM5; ab207718, Abcam, China; 1:300 dilution), anti-EGF receptor (EGFR; ab52894, Abcam, China; 1:600 dilution), and anti-stratifin (SFN; ab268067, Abcam, China; 1:800 dilution). Each antibody dilution was optimized through preliminary experiments. Tissue sections underwent standard deparaffinization and antigen retrieval protocols. Primary antibodies were incubated overnight at 4°C, followed by detection using the EnVision Detection System (Dako, Denmark). Appropriate positive and negative controls were included for each antibody. The Human Protein Atlas database (https://www.proteinatlas.org/) was used to validate the protein expression of the core genes.

2.9. Statistical analysis

All statistical analyses were performed using R version 4.4.1. For non-parametric data, the Wilcoxon test and Kruskal-Wallis test were used for comparing two independent samples and multiple samples, respectively. A $p<0.05$ was considered statistically significant. Related R packages, including "ggplot2," "ggpubr," "survival," "survminer," and others, were downloaded from Bioconductor or the R packages repository. Statistical significance for all analyses was set at $p<0.05$.

3. Results

3.1. Expression, mutation, and prognosis of ARGs in melanoma

A total of 813 normal skin samples and 471 SKCM samples were obtained from the TCGA and GTEx databases. In this study, 22 ARGs were included in the analysis, comprising seven high-risk genes and 15 low-risk genes (Figure 1A and B). To further explore the mutational characteristics of these ARGs in melanoma, somatic mutation analysis was performed. The results demonstrated that *PIK3CG* exhibited the highest mutation rate (7%), while *CEACAM5* and *EGFR* had mutation rates of 5%. The remaining ARGs displayed minimal or no mutations in melanoma (Figure 1C). CNV-related mutations were also common, with *MCL1*, *CEBPB*, and *MAP2K1* predominantly exhibiting amplification mutations, whereas *SFN*, *CASP3*, and Insulin-like growth factor 1 (*IGF1*) mutations showed predominantly deletion mutations (Figure 1D). CNV alterations across chromosomes were visualized to identify the genomic loci of affected ARGs (Figure 1E). Interaction, association, and prognostic analyses revealed that *IGF1*, *BCAR1*, *EGFR*, *CEACAM5*, Polo-like kinase 1 (*PLK1*), and *SFN* functioned as risk factors, while the remaining 16 ARGs served as protective factors. Most ARGs exhibited positive correlations with each other, although *BCAR1*, *CASP3*, *PLK1*, *SFN*, *PIK3CG*, *PTK2B*, and *CFLAR* showed negative correlations (Figure 1F).

3.2. Dataset batch correction and DEGs

We initially performed rigorous batch correction and integration of the GSE15605 and GSE3189 datasets. Post-correction results demonstrated high consistency between the two datasets (Figure 2A). Based on the integrated dataset, we conducted comprehensive differential gene expression analysis to reveal molecular-level changes between SKCM and control groups. The analysis identified a total of 3749 DEGs, including 1769 downregulated genes and 1980 upregulated genes. These key findings are detailed in Table S1. Heatmap visualization (Figure 2B) intuitively illustrates the distinct expression patterns of these DEGs between normal and tumor samples.

3.3. Model gene acquisition through 113 machine learning models

Through cross-analysis of DEGs and ARGs, we precisely identified nine key overlapping genes (Figure 3A). Subsequently, we constructed a comprehensive prediction framework encompassing 113 machine learning models and systematically evaluated classification performance across training and testing cohorts. Within this computational framework, the Elastic Net model (Enet[alpha=0.4]) emerged as the optimal classifier, achieving an exceptional average AUC of 0.959 (Figure 3B). Based on this model, we successfully identified eight key feature genes—*CEACAM5*, *CEACAM6*, *CEBPB*, *EGFR*, *IGF1*, *PLK1*, *SFN*, and *tissue inhibitor of metalloproteinase 1*. To comprehensively validate the diagnostic potential of these model genes, we performed rigorous ROC analyses in both the training cohort and independent validation sets. The results demonstrated that *CEACAM5*, *CEACAM6*, *CEBPB*, EGFR, *PLK1*, and *SFN* exhibited robust diagnostic performance across both cohorts, with AUC values consistently exceeding 0.7 (Figure 3C and D). These findings not only affirm the potential of these genes as diagnostic biomarkers but also provide important molecular insights for the precise diagnosis of SKCM.

3.4. Functional enrichment analysis of model genes

To elucidate the functional mechanisms of model genes in SKCM initiation and progression, we performed comprehensive bioinformatics functional enrichment analysis, including GO and KEGG analyses. GO functional enrichment analysis revealed that model genes were significantly involved in several key biological processes. At the biological process level, they were enriched in

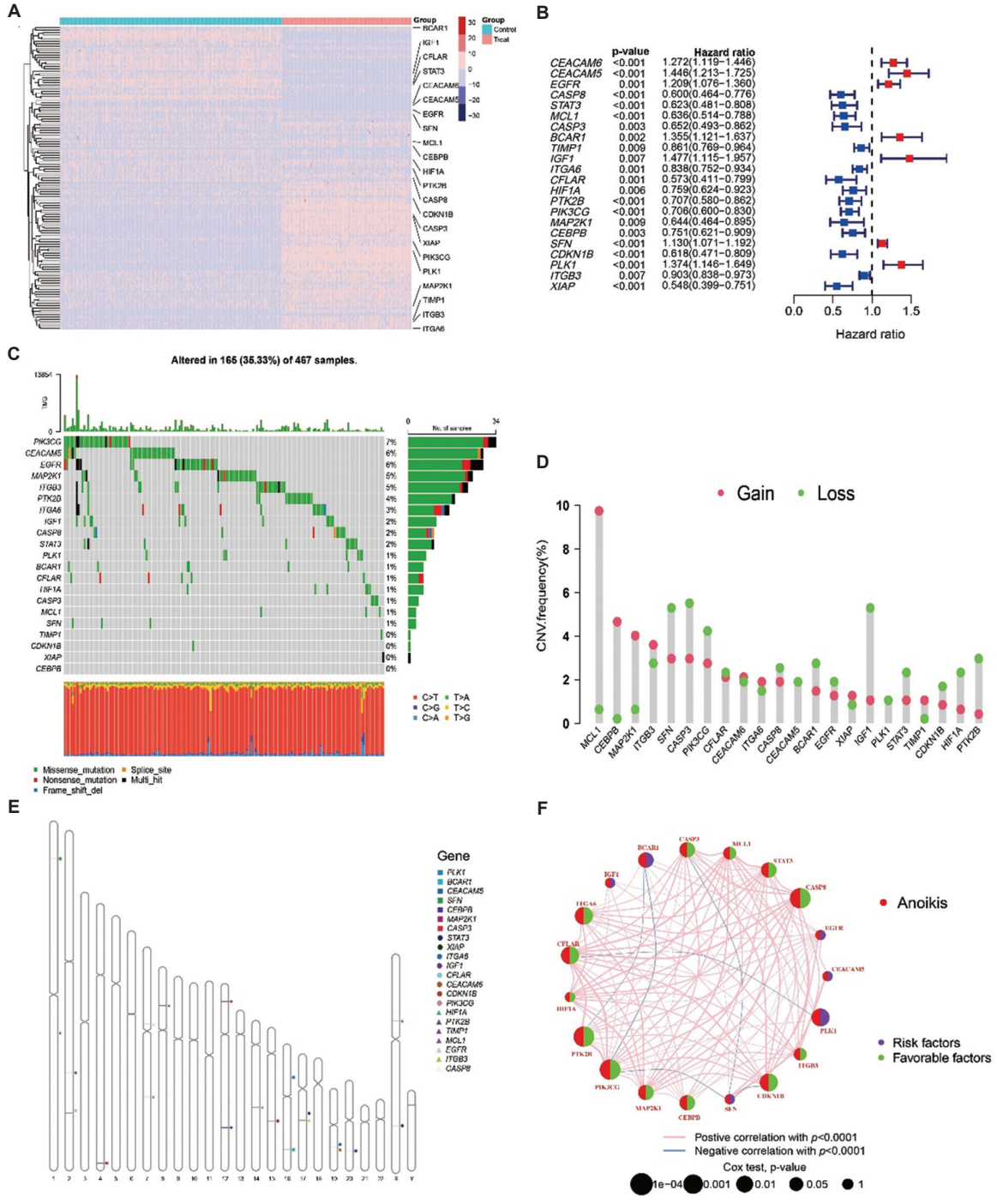

Figure 1. Genetic and expressional variations of anoikis-related genes (ARGs) in skin cutaneous melanoma (SKCM). (A) Expression of 22 ARGs in SKCM versus normal Tissue Samples. (B) Forest plot showing the association between ARGs and overall survival rates. (C) Mutation frequencies of 22 ARGs in 473 SKCM patients from The Cancer Genome Atlas (TCGA)-SKCM dataset. Each column represents an individual patient. The top bar graph displays tumor mutational burden. Right-side values indicate mutation frequencies per ARG. The adjacent bar chart shows the proportions of different mutation types. The stacked bar graph below illustrates mutation types per sample. (D) Copy number variation (CNV) frequencies of ARGs in TCGA-SKCM patients. (E) Genomic loci of CNV mutations in ARGs across the 23 chromosomes. (F) Interaction network of ARGs in SKCM. Circle size reflects the impact of each regulatory factor on prognosis, with significance levels ranging from $p<0.0001$ to $p<1$. Purple semicircles indicate unfavorable prognostic factors, while green semicircles represent protective factors. Connecting lines between regulators indicate interactions, with blue denoting negative correlations and red denoting positive correlations.
Abbreviations: del: Deletion; Multi: Multiple.

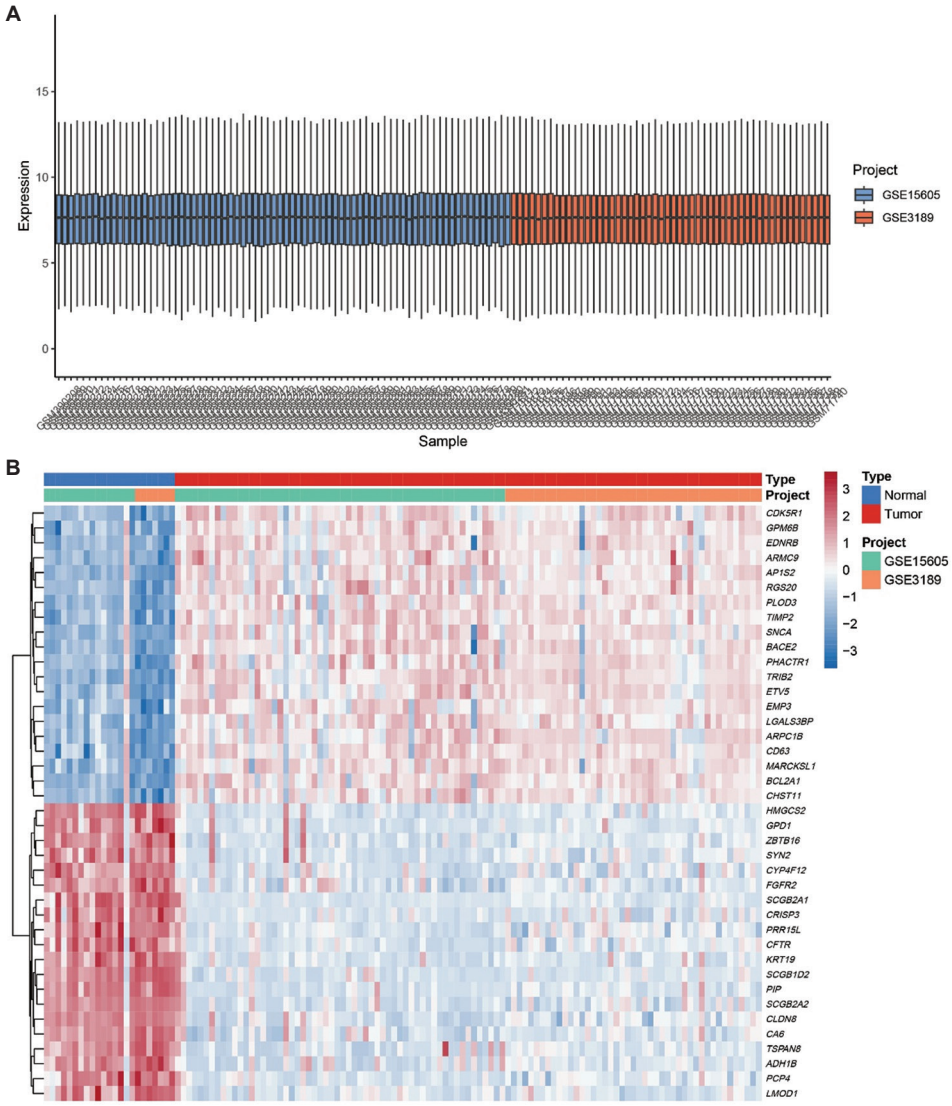

Figure 2. Data integration analysis before and after batch effect correction. (A) Expression data distribution after batch correction, showing successful elimination of systematic differences between datasets; expression profiles of the two datasets became consistent. (B) Heatmap of differentially expressed genes.

epithelial cell proliferation, regulation of protein kinase activity, and the neuron apoptotic process pathways. Cellular component and molecular function analyses further demonstrated enrichment in processes such as cell adhesion, cytoskeletal remodeling, and various key protein interactions (Figure 4A). KEGG pathway analysis further revealed the potential pathogenic mechanisms associated with these genes. The results showed that the model genes primarily participate in several critical signal transduction pathways, including human cytomegalovirus infection, the PI3K-Akt signaling pathway, and the hypoxia-inducible factor-1 signaling pathway (Figure 4B). These pathways are known to play crucial roles in tumorigenesis, progression, and metastasis.

3.5. Core gene identification

To thoroughly investigate the prognostic value of model genes in SKCM, we performed a comprehensive survival analysis. The study results revealed a critical prognostic pattern—high expression of *CEACAM5*, *CEACAM6*, *EGFR*, *PLK1*, and *SFN* was closely associated with significantly poorer OS rates in SKCM patients (Figure 5A-E). In contrast, high expression of *IGF1* and *CEBPB* appeared to confer certain survival advantages to patients (Figure 5F and G). These genes show varying degrees of association with clinical features in melanoma. *EGFR* expression significantly varied across tumor stages, *CEACAM5* expression was influenced by age, while the other genes showed no

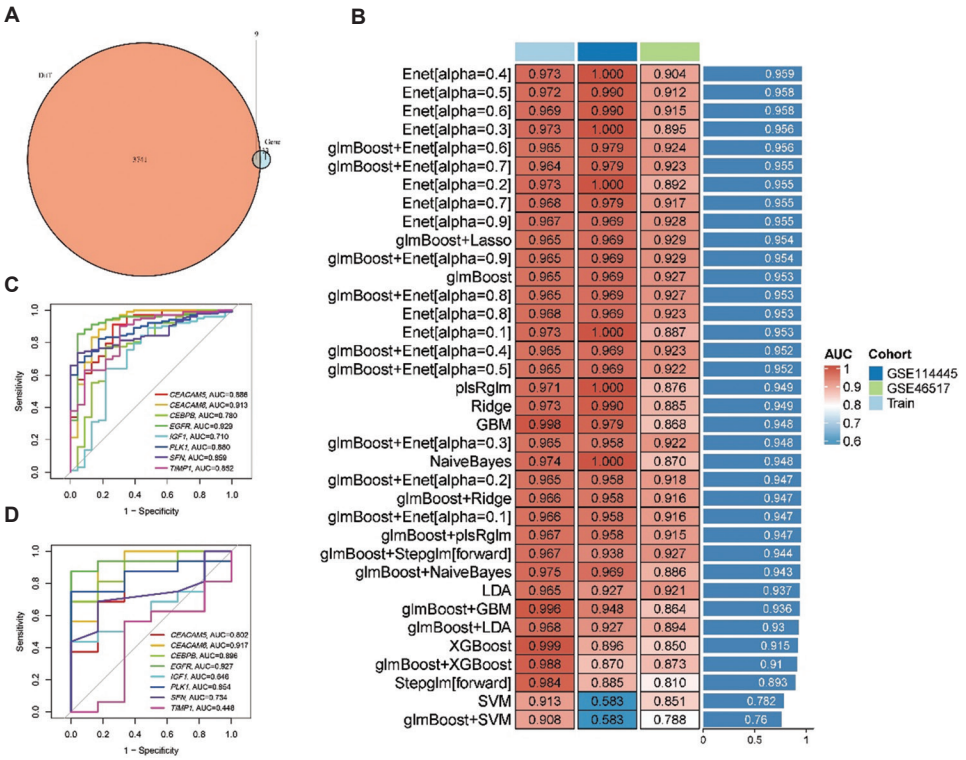

Figure 3. Machine learning model performance evaluation and comparison. (A) Venn diagram showing the intersection of differentially expressed genes and anoikis-related genes, yielding nine overlapping genes. (B) Performance heatmap of 113 machine learning algorithm combinations, displaying key performance metrics. (C) Receiver operating characteristic (ROC) curve for the training set. (D) ROC curve for the validation set.

Abbreviations: AUC: Area under the curve; diff: Difference; Enet: Elastic Net model; GBM: Gradient Boosting Machine; glmBoost: Generalized Linear Model Boosting; LDA: Linear Discriminant Analysis; plsRglm: Partial Least Squares Regression for Generalized Linear Models; XGBoost: Extreme Gradient Boosting; Stepglm: Stepwise Generalized Linear Model; SVM: Support Vector Machine.

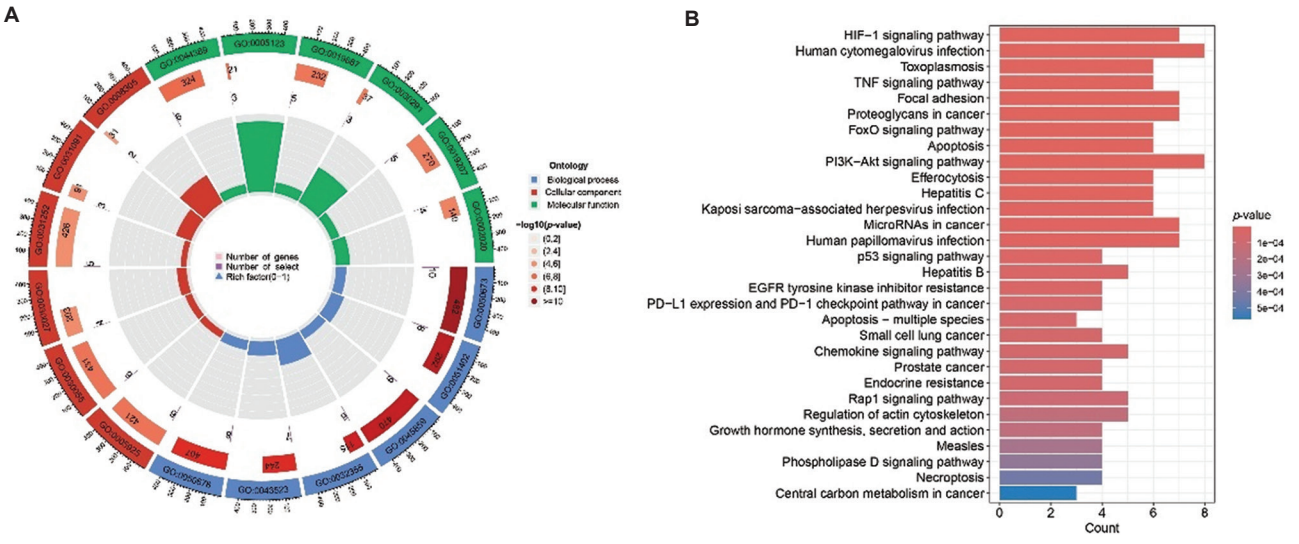

Figure 4. Functional enrichment analysis of model genes. (A) Gene Ontology functional enrichment analysis reveals the important roles of model genes in multiple key biological processes. (B) Kyoto Encyclopedia of Genes and Genomes pathway enrichment analysis shows that these genes are primarily involved in various cancer-related signaling pathways.

Abbreviations: Akt: Protein kinase B; EGFR: Epidermal growth factor receptor; FoxO: Forkhead box O; HIF-1: Hypoxia-inducible factor 1; PD-L1: Programmed death-ligand 1; PD-1: Programmed cell death protein 1; PI3K: Phosphoinositide 3-kinase; p53: Tumor protein p53; Rap1: Ras-associated protein 1; TNF: Tumor necrosis factor..

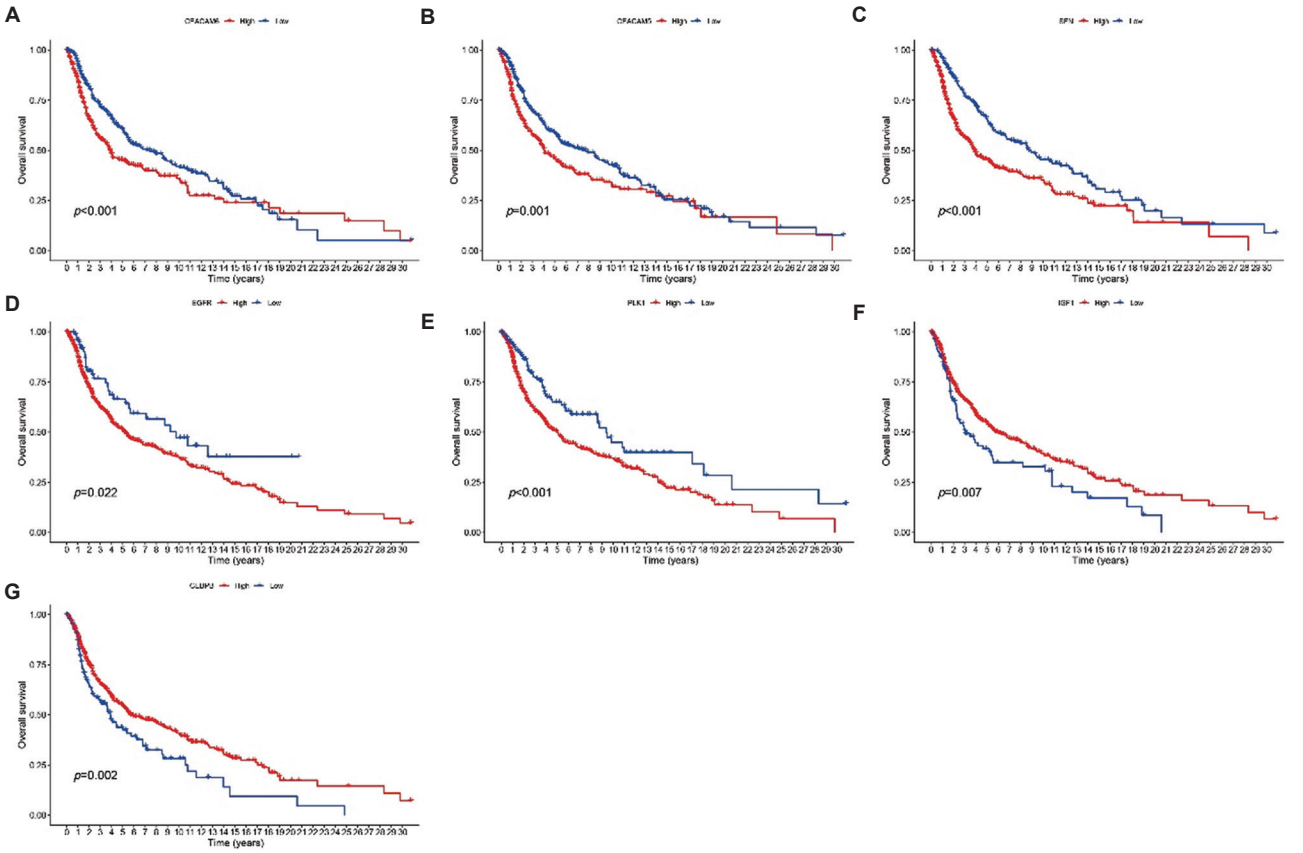

Figure 5. The Kaplan-Meier curves illustrate the overall survival of skin cutaneous melanoma (SKCM) patients with respect to anoikis-related genes (ARG) expression. (A-E) High expression of certain ARGs is associated with unfavorable prognosis in SKCM. These genes include *CEACAM6*, *CEACAM5*, *SFN*, *EGFR* and *PLK1*. (F and G) Low expression of specific ARGs is detrimental to SKCM survival. These genes include *IGF1* and *CEBPB*.
Abbreviations: CEACAM: Carcinoembryonic antigen-related cell adhesion molecule; CEBPB: CCAAT enhancer binding protein beta; EGFR: Epidermal growth factor receptor; IGF1: Insulin-like growth factor 1; PLK1: Polo-like kinase 1; SFN: Stratifin.

significant association with stage, gender, or age (Figure A1). PPI network analysis further validated these findings, highlighting *CEACAM5*, *CEACAM6*, *EGFR*, and *SFN* as key interconnected genes (Figure 6A and B). Through the integration of survival curve analysis and in-depth insights from protein interaction networks, we ultimately identified *CEACAM5*, *CEACAM6*, *EGFR*, *PLK1*, and *SFN* as core genes with important prognostic significance. These genes not only demonstrated statistically significant differences in survival analysis, but their complex interaction dynamics also highlighted their critical roles in melanoma initiation and development.

3.6. Correlation analysis between core genes and immune cell infiltration

Through quantitative assessment of immune cells in tumor samples using the CIBERSORT algorithm, we discovered significant correlations between core genes and multiple immune-infiltrating cells (Figure 7A). Correlation analysis of *CEACAM5* with immune cells showed significant associations with multiple immune cell subsets, including activated dendritic cells, T cells, and plasma cells (Figure 7B). Correlation analysis of *CEACAM6* revealed close associations with various immune cell types, including dendritic cells and plasma cells (Figure 7C). *EGFR* was particularly prominent in immune cell correlation analysis, showing significant correlations with T cell memory subsets, B cells, dendritic cells, and other immune cell types (Figure 7D). SFN is primarily positively correlated with activated dendritic cells, while negatively correlated with M1 macrophages (Figure 7E). Additionally, PLK1 shows a positive correlation mainly with M0 macrophages and resting NK cells, and a negative correlation with monocytes, regulatory T cells, plasma cells, and $CD8^+$ T cells (Figure 7E).

3.7. Combined ROC analysis and nomogram construction of core genes

To validate the diagnostic capability of the five core genes in SKCM, we performed a combined diagnostic ROC analysis

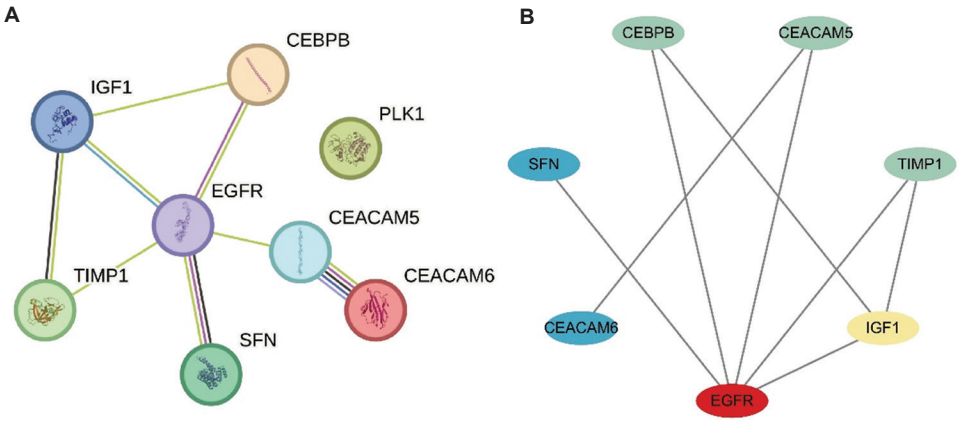

Figure 6. Protein-protein interaction network analysis of key genes. (A) Protein-protein interaction network constructed using the STRING database, showing interactions among CEBPB, IGF1, EGFR, PLK1, CEACAM5, CEACAM6, TIMP1, and SFN. Nodes represent proteins with different colors indicating distinct functional clusters. Edge thickness represents interaction confidence scores. The network reveals dense interconnections among these proteins, suggesting coordinated biological functions. (B) Simplified network diagram displaying the core interactions between the eight key proteins. Lines represent direct protein-protein interactions, with EGFR appearing as a central hub protein connecting multiple network components.
Abbreviations: CEACAM: Carcinoembryonic antigen-related cell adhesion molecule; CEBPB: CCAAT enhancer binding protein beta; EGFR: Epidermal growth factor receptor; IGF1: Insulin-like growth factor 1; PLK1: Polo-like kinase 1; SFN: Stratifin; TIMP1: Tissue inhibitor of metalloproteinase 1.

on both testing and validation sets. In the testing and training sets, the AUC values for the combined diagnosis of these five genes were 0.969 and 0.971, respectively (Figure 8A and B), demonstrating extremely high diagnostic accuracy and stability. This indicates that these genes possess strong potential for SKCM discrimination. The Clinical Impact Curve displayed changes in the number of high-risk patients under different risk thresholds (Figure 8C). Decision curve analysis showed that, compared to the "all" and "none" models, our gene model (red line) significantly improved the net benefit of clinical decision-making across a wide range of threshold probabilities (Figure 8D). The calibration curve demonstrated high concordance between model-predicted probabilities and actual outcomes (Figure 8E). The nomogram illustrated the potential of these five core genes as diagnostic biomarkers for SKCM, providing an important theoretical foundation for personalized risk assessment and precision medicine (Figure 8F).

3.8. Immunohistochemical validation of core genes

To comprehensively validate the expression characteristics of *CEACAM5*, *CEACAM6*, *EGFR*, *PLK1*, and *SFN* in SKCM, we performed in-depth immunohistochemical analysis. The results revealed significant expression of these key genes in tumor tissues (Figure 9A-E). These immunohistochemical findings not only confirmed the high expression of the five core genes in SKCM but also suggested their potential critical regulatory roles in tumor progression.

4. Discussion

This comprehensive study successfully identified and validated a five-gene anoikis-related signature (*CEACAM5*, *CEACAM6*, *EGFR*, *SFN*, and *PLK1*) with exceptional diagnostic and prognostic value in melanoma through the integration of multiple machine learning algorithms and multi-omics data analysis. Our findings provide new molecular targets for precise melanoma diagnosis and establish an important foundation for understanding the mechanistic role of anoikis resistance in melanoma development and progression.

Anoikis, a form of programmed cell death, is a crucial mechanism for maintaining normal tissue and organ homeostasis. It is primarily induced by the loss of cell-extracellular matrix interactions.[16] However, malignant tumor cells can evade this natural protective mechanism by acquiring anoikis resistance, thereby gaining invasive and metastatic capabilities.[17] In melanoma, several intracellular signaling cascades have been identified as potential drivers of anoikis resistance.[18] Simpson *et al.*[19] demonstrated that melanoma cells can effectively suppress anoikis through the activation of multiple survival signaling pathways, including PI3K/AKT and NF-κB pathways. Our findings are highly consistent with this perspective, as KEGG enrichment analysis revealed that the core genes identified in our study are primarily enriched in the PI3K-Akt signaling pathway, further validating the important role of anoikis resistance in melanoma. Multiple studies have shown that the acquisition of anoikis resistance in tumor cells can be driven through various pathways.[20-22]

The five-gene diagnostic panel identified in this study demonstrates strong potential for clinical translation, with significant advantages over current diagnostic approaches. Our machine learning-based signature

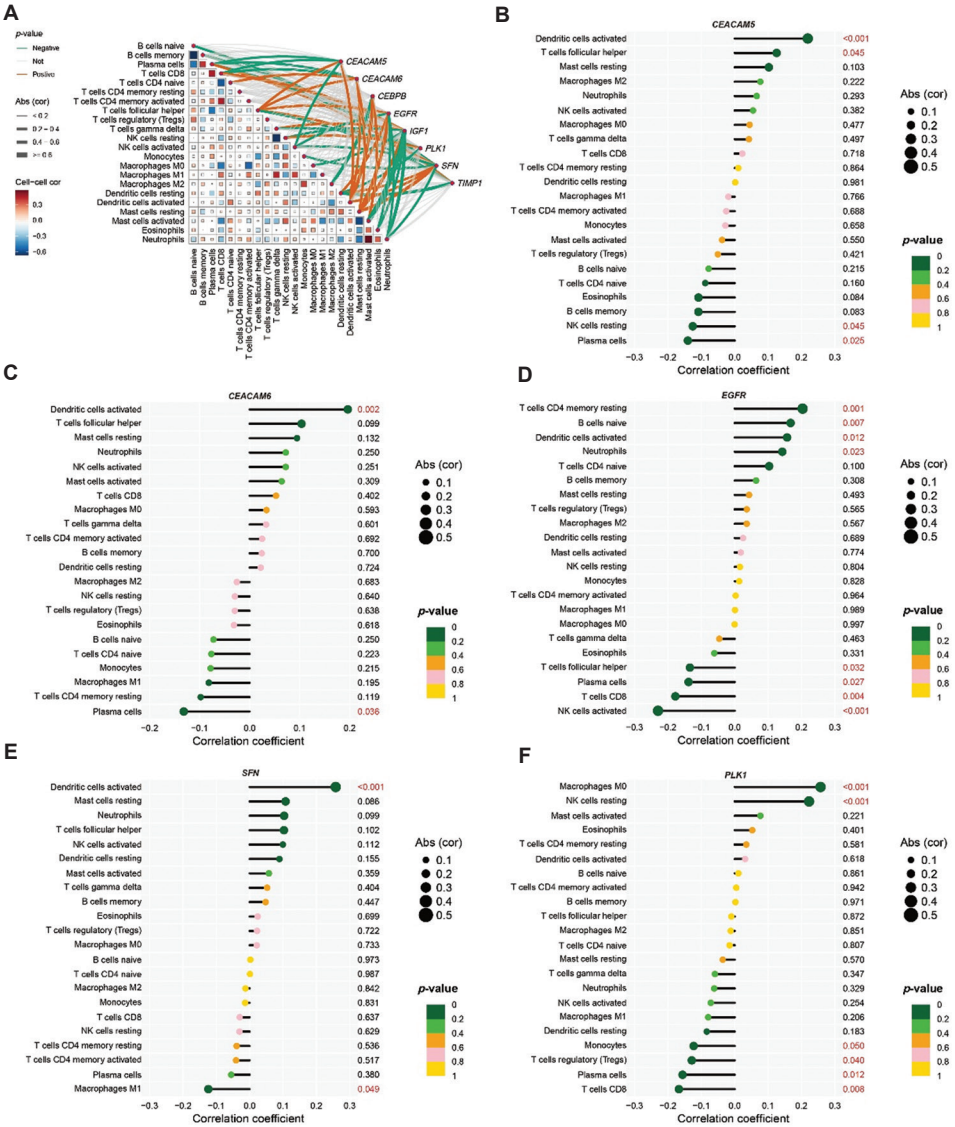

Figure 7. Correlation analysis between key genes and tumor-infiltrating immune cells. (A) Comprehensive correlation heatmap showing Spearman correlation coefficients between the eight key genes (*CEBPB*, *CEACAM5*, *CEACAM6*, *EGFR*, *IGF1*, *PLK1*, *SFN*, TIMP1) and 22 types of tumor-infiltrating immune cells. Cell-cell correlations are represented by color intensity, indicating correlation strength (blue: negative correlation, red: positive correlation). *p*-values are indicated by color coding. (B-F) Individual correlation plots for each key gene, showing their associations with different immune cell types. Each plot displays correlation coefficients on the x-axis, with dot size representing absolute correlation values and colors indicating statistical significance (*p*-values). Significant correlations ($p<0.05$) are highlighted, revealing distinct immune infiltration patterns associated with each gene.

Abbreviations: Abs: Absolute; CD: Cluster of differentiation; cor: Correlation; NK: Natural killer; CEACAM: Carcinoembryonic antigen-related cell adhesion molecule; CEBPB: CCAAT enhancer binding protein beta; EGFR: Epidermal growth factor receptor; IGF1: Insulin-like growth factor 1; PLK1: Polo-like kinase 1; SFN: Stratifin; TIMP1: Tissue inhibitor of metalloproteinase 1.

achieved outstanding diagnostic performance, with combined AUC values of 0.969 and 0.971 in the training and validation sets, respectively, substantially exceeding the performance of individual traditional biomarkers. This high diagnostic accuracy addresses a critical clinical need, as the current pathological diagnosis of melanoma relies heavily on morphological assessment and a limited panel of immunohistochemical markers, including S100, HMB-45, Melan-A, and sex-determining region Y-related high mobility group box-containing protein (SOX) 10.[23]

Recent studies have highlighted the diagnostic challenges posed by atypical melanocytic lesions, particularly in distinguishing early melanoma from

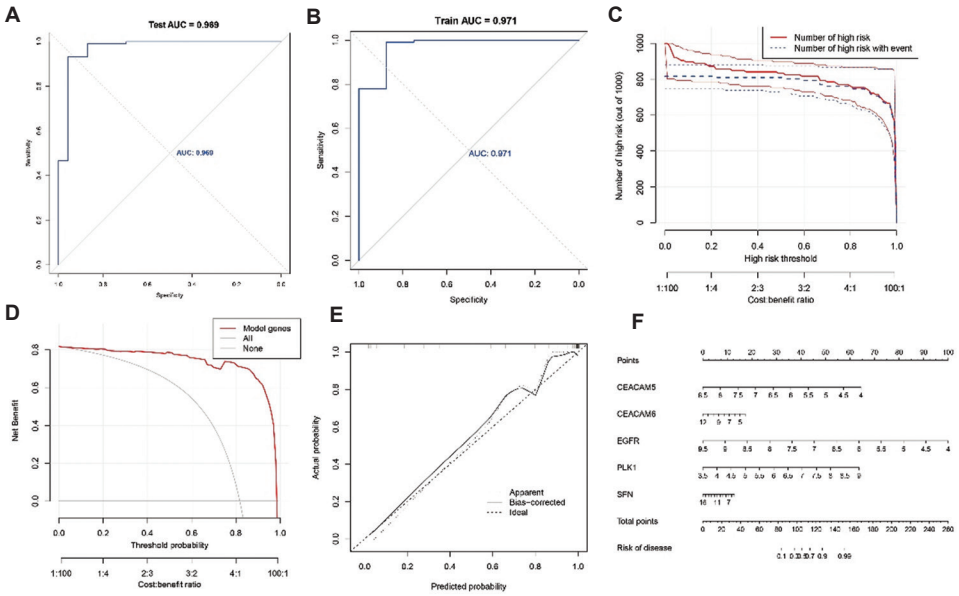

Figure 8. Performance evaluation and clinical utility assessment of the five-gene diagnostic model. (A) Receiver operating characteristic (ROC) curve analysis in the test dataset showing excellent discriminative performance of the five-gene model (*CEACAM5*, *CEACAM6*, *EGFR*, *PLK1*, and *SFN*) for skin cutaneous melanoma diagnosis. The model achieved an area under the curve (AUC) of 0.969. (B) ROC curve analysis in the validation dataset demonstrating robust model performance with an AUC of 0.971. (C) Clinical impact curve displaying the relationship between risk threshold probability and the number of high-risk patients. The upper panel shows the number of patients classified as high-risk (red solid line) and those experiencing events (red dashed line) across different threshold probabilities. The lower panel presents the cost-benefit ratio, aiding clinicians in determining optimal risk thresholds for clinical decision-making. (D) Decision curve analysis comparing the clinical utility of different strategies. The red line represents our five-gene model, while the gray and black lines represent the "treat all" and "treat none" strategies, respectively. (E) Calibration curve assessing the agreement between predicted probabilities and observed outcomes. The solid line represents the apparent performance, the dashed line indicates bias-corrected performance, and the dotted diagonal line reflects perfect calibration. (F) Nomogram for individualized risk assessment incorporating the five core genes (*CEACAM5*, *CEACAM6*, *EGFR*, *PLK1*, and *SFN*). Each gene contributes points based on its expression level, and the total score corresponding to the disease risk probability.

Abbreviations: CEACAM: Carcinoembryonic antigen-related cell adhesion molecule; EGFR: Epidermal growth factor receptor; PLK1: Polo-like kinase 1; SFN: Stratifin.

dysplastic nevi and other melanoma mimics.[24] Elmore *et al.*[25] demonstrated significant inter-observer variability in melanoma diagnosis, with agreement rates as low as 64% for borderline lesions. Our quantitative gene expression-based approach offers the potential to reduce such diagnostic uncertainty by providing objective, reproducible molecular measurements that complement traditional histopathological assessment.

Our survival analysis revealed that high expression of all five core genes was significantly associated with poor patient prognosis, establishing their dual utility as both diagnostic and prognostic biomarkers. This finding is particularly important given the heterogeneous clinical behavior of melanoma and the pressing need for accurate prognostic stratification to guide treatment decisions.[26]

The prognostic value of individual genes within our signature is supported by extensive literature. *EGFR* overexpression has been consistently associated with poor outcomes in multiple cancer types, including melanoma.[27] Similarly, *PLK1* overexpression has been identified as an independent poor prognostic factor across various malignancies,[28] with high *PLK1* expression significantly correlating with reduced OS and increased recurrence risk.[29]

Our research revealed that *CEACAM5* and *CEACAM6* are significantly overexpressed in melanoma and closely associated with poor patient prognosis. The CEACAM family represents an important class of cell surface glycoproteins that exert complex regulatory functions in tumor biology.[30] In their comprehensive review, Beauchemin and Arabzadeh noted that CEACAM molecules may play dual roles as either tumor promoters or suppressors, depending on the cancer types.[31] In colorectal cancer, high *CEACAM5* expression is significantly associated with tumor invasiveness and metastatic potential.[32] More importantly, recent studies have indicated that CEACAM6 is linked to anoikis resistance and increased metastasis.[33]

The prognostic stratification achieved by our five-gene signature enables the identification of high-risk

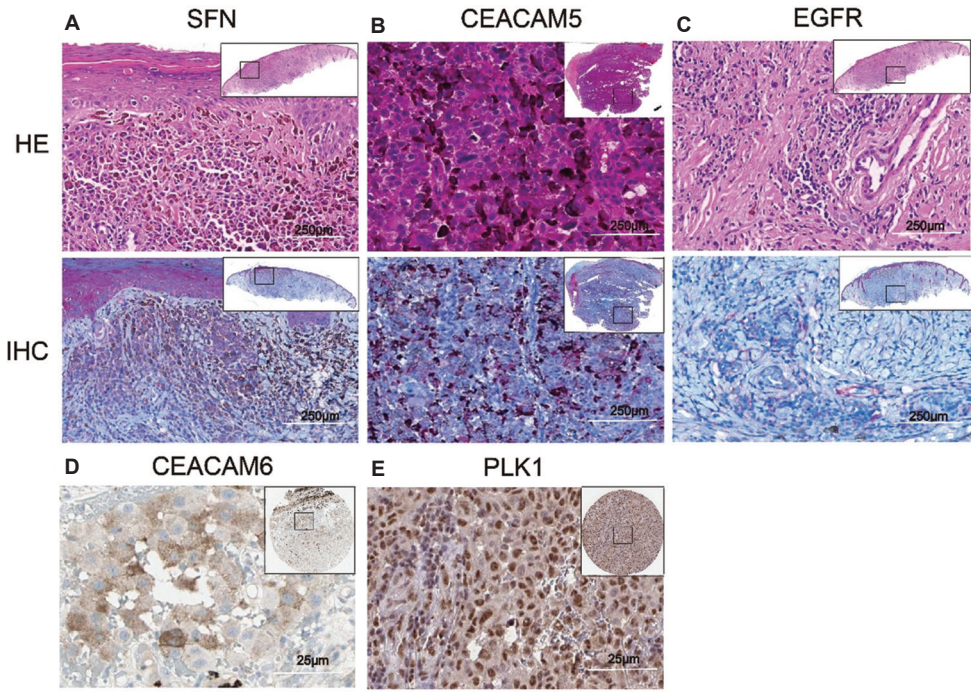

Figure 9. Histopathological validation of five core genes in skin cutaneous melanoma tissues. (A) The hematoxylin and eosin (HE) image reveals disorganized melanoma cells in the dermis. Immunohistochemistry (IHC) staining shows strong cytoplasmic positivity for stratifin in melanoma cells, especially concentrated in the tumor nest region. (B) The HE staining displays high cellular density and pleomorphism. (C) HE staining reveals fibrotic stroma and infiltrative tumor growth. IHC shows moderate epidermal growth factor receptor (EGFR) staining in tumor cells with a membranous pattern, suggesting EGFR involvement in melanoma progression. (D) IHC analysis shows focal and cytoplasmic staining of carcinoembryonic antigen-related cell adhesion molecule 6 in tumor cells, supporting its overexpression in selected melanoma cell populations. (E) IHC staining shows strong nuclear positivity of polo-like kinase 1 (PLK1) in melanoma cells, consistent with its role in cell proliferation. The inset highlights a high PLK1 expression pattern within the tumor core. Scale bars: (A-C) = 250 μm, (D and E) = 25 μm; Magnifications: (A-C) = ×20, (D and E) = ×40.

patients who may benefit from more aggressive treatment approaches or closer surveillance protocols. Contemporary melanoma management increasingly relies on molecular profiling for treatment selection, particularly in the context of targeted therapy and immunotherapy. Our signature provides additional stratification capability that could inform clinical decision-making and patient counseling regarding prognosis and treatment options.

The identification of therapeutically targetable genes within our signature opens new avenues for melanoma treatment development. Each of the five core genes represents a potential therapeutic target with existing or emerging targeted agents.

EGFR, another core gene identified in our study, plays a crucial role in melanoma development and progression. Abnormal activation of the EGFR signaling pathway represents a key mechanism through which various malignant tumors acquire resistance to anoikis.[34] Que *et al.*[35] demonstrated that in melanoma, *EGFR* overexpression significantly enhances tumor cell survival and anoikis resistance by activating downstream PI3K/AKT and MAPK signaling pathways. Furthermore, clinical trial data from Nathanson *et al.*[36] indicated that EGFR inhibitors show therapeutic efficacy in melanoma treatment, especially in patients with high *EGFR* expression, providing important translational value for our identification of *EGFR* as a diagnostic marker.

PLK1 and SFN (14-3-3 protein σ), as important cell cycle regulatory factors, also demonstrated significant diagnostic and prognostic value in our study. PLK1 is a critical regulator of cell cycle progression, and its abnormal expression is closely associated with the development of multiple tumors.[28] Mechanistic studies by Liu and Erikson[37] demonstrated that PLK1 effectively inhibits anoikis in tumor cells by phosphorylating several key apoptosis-regulatory proteins. In melanoma, Cholewa *et al.*[38] discovered that PLK1 likely plays an active role in oncogenic transformation. SFN, an important member of the 14-3-3 protein family, plays a crucial role in cell cycle checkpoint control and the regulation of apoptosis.[39] Research by Benzinger *et al.*[40] revealed that SFN can effectively inhibit the initiation of cellular apoptotic programs by binding

to various pro-apoptotic proteins. These findings provide important mechanistic explanations for our observations of high *PLK1* and *SFN* expression in melanoma and their association with poor prognosis.

Our immune cell infiltration analysis revealed close associations between core genes and the tumor immune microenvironment, a finding with important clinical implications. As a highly immunogenic tumor, the characteristics of the immune microenvironment in melanoma provide valuable guidance for both diagnosis and treatment.[7] Research by Gajewski *et al.*[41] demonstrated that the composition and functional status of the tumor immune microenvironment are key factors affecting melanoma patient prognosis and treatment response.

The significant correlation we observed between EGFR and memory T-cell subsets is particularly noteworthy. Memory T cells play an important role in anti-tumor immunity, and their infiltration levels are closely associated with long-term patient survival.[42] In addition, the correlation between CEACAM5 and dendritic cells also carries significant implications.[43] These findings not only provide new perspectives for understanding the role of core genes in melanoma immune evasion but also offer important insights for developing personalized treatment strategies based on immunotherapy.

The five-gene diagnostic panel identified in this study demonstrates substantial potential for clinical translation. Current pathological diagnosis of melanoma primarily relies on morphological assessment and a limited set of immunohistochemical markers, presenting diagnostic challenges in certain atypical cases.[44] Our diagnostic model, based on ARGs, provides clinicians with an intuitive, quantitative diagnostic tool in the form of a nomogram, which has the potential to significantly improve the accuracy and consistency of melanoma diagnosis.

From a therapeutic perspective, the core genes we identified also offer new opportunities for targeted therapy. EGFR inhibitors have demonstrated efficacy in the treatment of various tumors,[45] while PLK1 inhibitors, as emerging anti-tumor agents, have shown promising prospects in clinical trials.[46] Furthermore, immunotherapy strategies targeting the CEACAM family are also being actively explored.

While our study provides robust evidence for the diagnostic and prognostic value of the five-gene anoikis signature, several limitations should be acknowledged and addressed in future research. The immunohistochemical validation was performed on a relatively limited sample size, which constrains the generalizability of our protein-level findings. Although we employed multiple validation strategies, including cross-platform verification using the Human Protein Atlas database and validation across multiple independent transcriptomic datasets, larger multi-center clinical validation studies are needed to confirm the clinical utility of our signature. Future studies should incorporate diverse patient populations from various geographic regions and clinical centers to ensure broad applicability. Furthermore, we plan to expand future research by including additional experiments, such as *in vitro* anoikis resistance models, molecular mechanism investigations, integrative mechanistic studies, *in vivo* validation, and clinical correlation analyses.

While our study provides extensive computational evidence for the role of the identified genes in anoikis resistance, direct functional validation through experimental approaches is needed to confirm mechanistic relationships. Future research should include: (i) *in vitro* anoikis resistance assays using melanoma cell lines with genetic modulation of the target genes; (ii) validation of five biomarker genes across different melanoma subtypes; (iii) *in vivo* metastasis models to evaluate the impact of gene expression on metastatic colonization, and (iv) mechanistic studies to elucidate-specific molecular pathways involved in anoikis resistance.

Melanoma exhibits significant intra-tumoral heterogeneity, which may impact the consistency of biomarker expression. Our analysis was based on bulk tissue samples, which may not fully capture the cellular diversity within tumors. Single-cell RNA sequencing approaches could provide more detailed insights into gene expression patterns across different cellular populations within melanoma tissues. Translation of our findings into clinical practice will require standardization of assay methodologies, the establishment of appropriate cutoff values, and integration with existing diagnostic workflows. Prospective clinical studies are also necessary to evaluate the performance of our gene signature in real-world diagnostic settings and to assess its impact on clinical decision-making and patient outcomes.

5. Conclusion

This study successfully identified five anoikis-related diagnostic biomarkers for melanoma—*CEACAM5*, *CEACAM6*, *EGFR*, *SFN*, and *PLK1*—through an innovative multi-algorithm machine learning strategy. These genes not only demonstrate excellent diagnostic performance but also provide new insights into melanoma pathogenesis through their critical roles in anoikis resistance and immune microenvironment regulation. As precision medicine advances, molecular diagnostics based on multi-gene panels will become an increasingly important direction

in tumor pathology. Our research makes a significant contribution to this emerging field by establishing a robust biomarker signature with potential clinical applications in melanoma diagnosis and therapeutic development.

Acknowledgments

None.

Funding

None.

Conflict of interest

The authors declare that they have no conflicts of interest.

Author contributions

Conceptualization: Jinchao Zhu
Data curation: All authors
Formal analysis: Jinchao Zhu
Writing–original draft: Tengfei Wang
Writing–review & editing: All authors

Ethics approval and consent to participate

Not applicable.

Consent for publication

Not applicable.

Availability of data

The datasets used in this study are available in online repositories. SKCM datasets were obtained from The Cancer Genome Atlas, including transcriptomic matrices and clinical information for skin cutaneous melanoma (SKCM; n=471) and normal tissue (n=1). Normal skin tissue expression data were sourced from the Genotype-Tissue Expression portal (https://gtexportal.org/home/). The GSE3189, GSE15605, GSE19234, GSE65904, and GSE66839 datasets, all of which include available OS data, were retrieved from the public Gene Expression Omnibus database. Autophagy-related genes were obtained from GeneCards (https://www.genecards.org/).

References

1. Davis LE, Shalin SC, Tackett AJ. Current State of melanoma diagnosis and treatment. *Cancer Biol Ther*. 2019;20(11):1366-1379.

   doi: 10.1080/15384047.2019.1640032

2. Nurla LA, Wafi G, Tatar R, *et al*. Recent-onset melanoma and the implications of the excessive use of tanning devices-case report and review of the literature. *Medicina (Kaunas)*. 2024;60(1):187.

   doi: 10.3390/medicina60010187

3. Apalla Z, Lallas A, Sotiriou E, Lazaridou E, Ioannides D. Epidemiological trends in skin cancer. *Dermatol Pract Concept*. 2017;7(2):1-6.

   doi: 10.5826/dpc.0702a01

4. Liu-Smith F, Ziogas A. Age-dependent interaction between sex and geographic ultraviolet index in melanoma risk. *J Am Acad Dermatol*. 2020;82(5):1102-1108.e3.

   doi: 10.1016/j.jaad.2017.11.049

5. Alhazmi R, Tong S, Darwish S, *et al*. Bis-cinnamamide derivatives as APE/Ref-1 inhibitors for the treatment of human melanoma. *Molecules*. 2022;27(9):2672.

   doi: 10.3390/molecules27092672

6. Huang YJ, Gao Y, Wang CJ, *et al*. Hydroxyurea regulates the development and survival of B16 melanoma cells by upregulating MiR-7013-3p. *Int J Med Sci*. 2021;18(8):1877-1885.

   doi: 10.7150/ijms.52177

7. Tumeh PC, Harview CL, Yearley JH, *et al*. PD-1 blockade induces responses by inhibiting adaptive immune resistance. *Nature*. 2014;515(7528):568-571.

   doi: 10.1038/nature13954

8. Ashrafizadeh M, Mohammadinejad R, Tavakol S, Ahmadi Z, Roomiani S, Katebi M. Autophagy, anoikis, ferroptosis, necroptosis, and endoplasmic reticulum stress: Potential applications in melanoma therapy. *J Cell Physiol*. 2019;234(11):19471-19479.

   doi: 10.1002/jcp.28740.

9. Yu LG. Cancer cell resistance to anoikis: MUC1 glycosylation comes to play. *Cell Death Dis*. 2017;8(7):e2962.

   doi: 10.1038/cddis.2017.363

10. Frisch SM, Screaton RA. Anoikis mechanisms. *Curr Opin Cell Biol*. 2001;13(5):555-562.

    doi: 10.1016/s0955-0674(00)00251-9

11. Raeisi M, Zehtabi M, Velaei K, Fayyazpour P, Aghaei N, Mehdizadeh A. Anoikis in cancer: The role of lipid signaling. *Cell Biol Int*. 2022;46(11):1717-1728.

    doi: 10.1002/cbin.11896

12. Jiang G, Song C, Wang X, *et al.* The multi-omics analysis identifies a novel cuproptosis-anoikis-related gene signature in prognosis and immune infiltration characterization of lung adenocarcinoma. *Heliyon*. 2023;9(3):e14091.

    doi: 10.1016/j.heliyon.2023.e14091

13. Juan Z, Dake C, Tanaka K, Shuixiang H. EGFL7 as a novel therapeutic candidate regulates cell invasion and anoikis in colorectal cancer through PI3K/AKT signaling pathway. *Int J Clin Oncol*. 2021;26(6):1099-1108.

doi: 10.1007/s10147-021-01888-x

14. Yuan H, Xu R, Li S, *et al.* The malignant transformation of viral hepatitis to hepatocellular carcinoma: Mechanisms and interventions. *MedComm (2020)*. 2025;6(3):e70121.

doi: 10.1002/mco2.70121

15. Zhu Z, Fang C, Xu H, *et al*. Anoikis resistance in diffuse glioma: The potential therapeutic targets in the future. *Front Oncol*. 2022;12:976557.

doi: 10.3389/fonc.2022.976557

16. Wang J, Luo Z, Lin L, *et al.* Anoikis-associated lung cancer metastasis: Mechanisms and therapies. *Cancers (Basel)*. 2022;14(19):4791.

doi: 10.3390/cancers14194791

17. Paoli P, Giannoni E, Chiarugi P. Anoikis molecular pathways and its role in cancer progression. *Biochim Biophys Acta*. 2013;1833(12):3481-3498.

doi: 10.1016/j.bbamcr.2013.06.026

18. Neuendorf HM, Simmons JL, Boyle GM. Therapeutic targeting of anoikis resistance in cutaneous melanoma metastasis. *Front Cell Dev Biol*. 2023;11:1183328.

doi: 10.3389/fcell.2023.1183328

19. Simpson CD, Anyiwe K, Schimmer AD. Anoikis resistance and tumor metastasis. *Cancer Lett*. 2008;272(2):177-185.

doi: 10.1016/j.canlet.2008.05.029

20. Song J, Liu Y, Liu F, *et al.* The 14-3-3σ protein promotes HCC anoikis resistance by inhibiting EGFR degradation and thereby activating the EGFR-dependent ERK1/2 signaling pathway. *Theranostics*. 2021;11(3):996-1015.

doi: 10.7150/thno.51646

21. Yu L, Wang X, Du Y, Zhang X, Ling Y. FASN knockdown inhibited anoikis resistance of gastric cancer cells via P-ERK1/2/Bcl-xL pathway. *Gastroenterol Res Pract*. 2021;2021:6674204.

doi: 10.1155/2021/6674204

22. Adeshakin FO, Adeshakin AO, Afolabi LO, Yan D, Zhang G, Wan X. Mechanisms for modulating anoikis resistance in cancer and the relevance of metabolic reprogramming. *Front Oncol*. 2021;11:626577.

doi: 10.3389/fonc.2021.626577

23. Helbig D. Hemato-oncological diseases as risk factor for recurrence or metastasis of pleomorphic dermal sarcoma. *Front Oncol*. 2022;12:873771.

doi: 10.3389/fonc.2022.873771

24. Piepkorn MW, Barnhill RL, Elder DE, *et al.* The MPATH-Dx reporting schema for melanocytic proliferations and melanoma. *J Am Acad Dermatol*. 2014;70(1):131-141.

doi: 10.1016/j.jaad.2013.07.027

25. Elmore JG, Barnhill RL, Elder DE, *et al.* Pathologists' diagnosis of invasive melanoma and melanocytic proliferations: Observer accuracy and reproducibility study. *BMJ*. 2017;357:j2813.

doi: 10.1136/bmj.j2813

26. Gershenwald JE, Scolyer RA, Hess KR, *et al.* Melanoma staging: Evidence-based changes in the American joint committee on cancer eighth edition cancer staging manual. *CA A Cancer J Clin*. 2017;67(6):472-492.

doi: 10.3322/caac.21409

27. Lee KH, Suh HY, Lee MW, Lee WJ, Chang SE. Prognostic significance of epidermal growth factor receptor expression in distant metastatic melanoma from primary cutaneous melanoma. *Ann Dermatol*. 2021;33(5):432-439.

doi: 10.5021/ad.2021.33.5.432

28. Strebhardt K. Multifaceted polo-like kinases: Drug targets and antitargets for cancer therapy. *Nat Rev Drug Discov*. 2010;9(8):643-660.

doi: 10.1038/nrd3184

29. Moore XTR, Gheghiani L, Fu Z. The role of polo-like kinase 1 in regulating the forkhead box family transcription factors. *Cells*. 2023;12(9):1344.

doi: 10.3390/cells12091344

30. Hammarström S. The carcinoembryonic antigen (CEA) family: Structures, suggested functions and expression in normal and malignant tissues. *Semin Cancer Biol*. 1999;9(2):67-81.

doi: 10.1006/scbi.1998.0119

31. Beauchemin N, Arabzadeh A. Carcinoembryonic antigen-related cell adhesion molecules (CEACAMs) in cancer progression and metastasis. *Cancer Metastasis Rev*. 2013;32(3-4):643-671.

doi: 10.1007/s10555-013-9444-6

32. Northrop-Albrecht EJ, Kim Y, Taylor WR, Majumder S, Kisiel JB, Lucien F. The proteomic landscape of stool-derived extracellular vesicles in patients with pre-cancerous lesions and colorectal cancer. *Commun Biol*. 2025;8(1):228.

doi: 10.1038/s42003-025-07652-5

33. Lee H, Jang Y, Park S, *et al.* Development and evaluation of a CEACAM6-targeting theranostic nanomedicine for photoacoustic-based diagnosis and chemotherapy of metastatic cancer. *Theranostics*. 2018;8(15):4247-4261.

doi: 10.7150/thno.25131

34. Dai Y, Zhang X, Ou Y, *et al*. Anoikis resistance--protagonists of breast cancer cells survive and metastasize after ECM detachment. *Cell Commun Signal*. 2023;21(1):190.

doi: 10.1186/s12964-023-01183-4

35. Que Z, Luo B, Yu P, *et al*. Polyphyllin VII induces CTC

anoikis to inhibit lung cancer metastasis through EGFR pathway regulation. *Int J Biol Sci*. 2023;19(16):5204-5217.

doi: 10.7150/ijbs.83682

36. Nathanson KL, Martin AM, Wubbenhorst B, *et al*. Tumor genetic analyses of patients with metastatic melanoma treated with the BRAF inhibitor dabrafenib (GSK2118436). *Clin Cancer Res*. 2013;19(17):4868-4878.

doi: 10.1158/1078-0432.Ccr-13-0827

37. Liu X, Erikson RL. Polo-like kinase (Plk)1 depletion induces apoptosis in cancer cells. *Proceed Natl Acad Sci United States Am*. 2003;100(10):5789-5794.

doi: 10.1073/pnas.1031523100

38. Cholewa BD, Liu X, Ahmad N. The role of polo-like kinase 1 in carcinogenesis: Cause or consequence? *Cancer Res*. 2013;73(23):6848-6855.

doi: 10.1158/0008-5472.Can-13-2197

39. Hermeking H. The 14-3-3 cancer connection. *Nat Rev Cancer*. 2003;3(12):931-943.

doi: 10.1038/nrc1230

40. Benzinger A, Muster N, Koch HB, Yates JR 3rd, Hermeking H. Targeted proteomic analysis of 14-3-3 sigma, a p53 effector commonly silenced in cancer. *Mol Cell Proteomics*. 2005;4(6):785-795.

doi: 10.1074/mcp.M500021-MCP200

41. Gajewski TF, Schreiber H, Fu YX. Innate and adaptive immune cells in the tumor microenvironment. *Nat Immunol*. 2013;14(10):1014-1022.

doi: 10.1038/ni.2703

42. Sayitoglu EC, Luca BA, Boss AP, *et al*. AML/T cell interactomics uncover correlates of patient outcomes and the key role of ICAM1 in T cell killing of AML. *Leukemia*. 2024;38(6):1246-1255.

doi: 10.1038/s41375-024-02255-1

43. Li Y, Gao Y, Chu W, Lv J, Li Z, Shi T. Differences in and verification of genetic alterations in chemotherapy and immunotherapy for metastatic melanoma. *Aging (Albany NY)*. 2021;13(20):23672-23688.

doi: 10.18632/aging.203640

44. Saliba E, Bhawan J. Aberrant expression of immunohistochemical markers in malignant melanoma: A review. *Dermatopathology (Basel)*. 2021;8(3):359-370.

doi: 10.3390/dermatopathology8030040

45. Azorin P, Bonin F, Tariq Z, *et al*. Kindlin-1 modulates the EGFR pathway and predicts sensitivity to EGFR inhibitors across cancer types. *Clin Transl Med*. 2022;12(4):e813.

doi: 10.1002/ctm2.813

46. Sinha N, Shen X, Haag J, *et al*. Onvansertib exhibits anti-proliferative and anti-invasive effects in endometrial cancer. *Front Pharmacol*. 2025;16:1545038.

doi: 10.3389/fphar.2025.1545038

Appendix

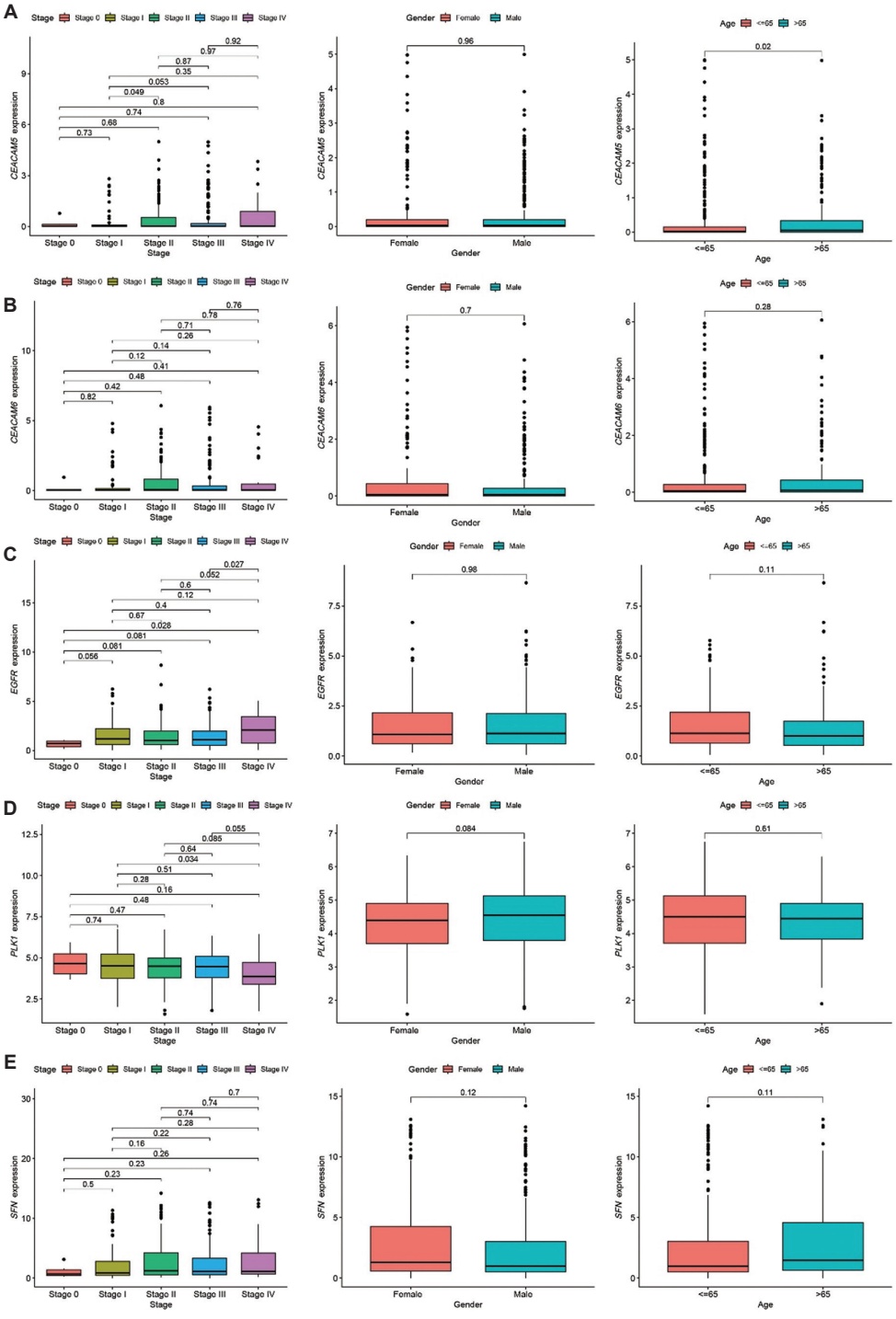

Figure A1. Expression levels of five core genes (*CEACAM5*, *CEACAM6*, *EGFR*, *PLK1*, and *SFN*) were analyzed in melanoma patients. (A) *CEACAM5* showed no significant difference in expression across tumor stages; however, a statistically significant difference was observed between age groups (p = 0.02), suggesting that age may influence *CEACAM5* expression. (B) *CEACAM6* showed no significant expression differences among tumor stages, genders, or age groups. (C) *EGFR* expression differed significantly across tumor stages (with some pairwise comparisons yielding p<0.05), indicating that *EGFR* expression changes with disease progression; however, no significant differences were observed between genders or age groups. (D) *PLK1* expression showed no significant differences across tumor stages, genders, or age groups. (E) *SFN* expression showed no significant differences across tumor stages, genders, or age groups.

Abbreviations: CEACAM: Carcinoembryonic antigen-related cell adhesion molecule; EGFR: Epidermal growth factor receptor; PLK1: Polo-like kinase 1; SFN: Stratifin